Copyright WILEY-VCH Verlag GmbH & Co. KGaA, 69469 Weinheim, Germany, 2015.

NANO MICRO small

Supporting Information

for *Small*, DOI: 10.1002/smll.201502398

Quantification of Protein-Induced Membrane Remodeling Kinetics In Vitro with Lipid Multilayer Gratings

*Troy W. Lowry, Hanaa Hariri, Plengchart Prommapan, Aubrey Kusi-Appiah, Nicholas Vafai, Ewa A. Bienkiewicz, David H. Van Winkle, Scott M. Stagg, and Steven Lenhert**

WILEY-VCH

Copyright WILEY-VCH Verlag GmbH & Co. KGaA, 69469 Weinheim, Germany, 2013.

Supporting Information

Quantification of Membrane Binding Protein Activity In Vitro with Lipid Multilayer Gratings

Troy W. Lowry, Hanaa Hariri, Plengchart Prommapan, Aubrey Kusi-Appiah, Nicholas Vafai, Ewa A. Bienkiewicz, David Van Winkle, Scott M. Stagg, Steven Lenhert

Supporting Material

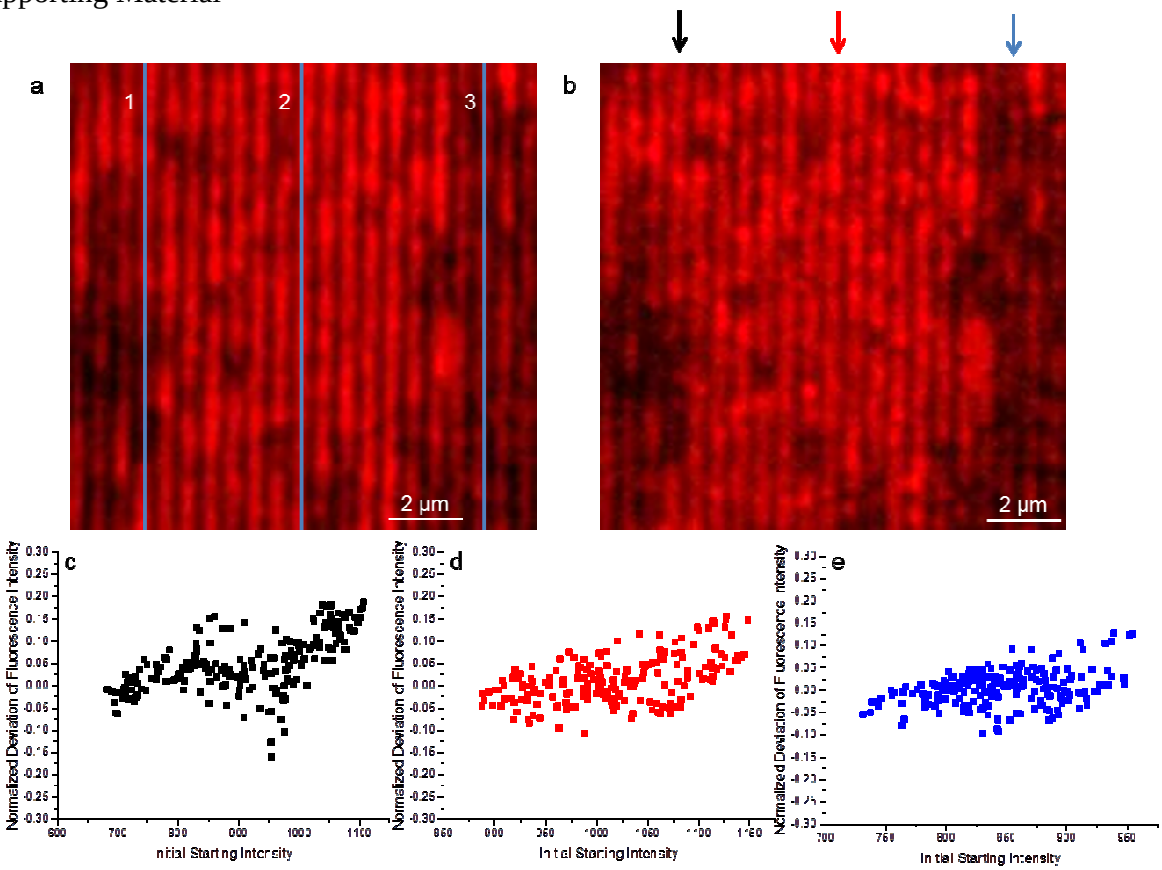

S. Figure 1. Lipid multilayer dewetting resulting from interaction with Sar1 is height dependent. (a) High magnification fluorescence image of lipid multilayer gratings before incubation with Sar1. (b) Lipid multilayer gratings after 25 minutes incubation with 10 µM Sar1. (c), (d) and (e): Normalized deviation for each pixel along the line scans shown in *a* and *b*. The data was normalized first to the highest intensity in each data set to account for any bleaching effects, then the incubated intensity *b* was subtracted from the initial intensity *a* and then divided by *a* to describe how the incubated intensity deviated from the starting intensity. Each line section shows that, when plotted as a function of the pixels initial starting intensity, the higher-intensity lipid grating lines deviate more than the lower intensities.

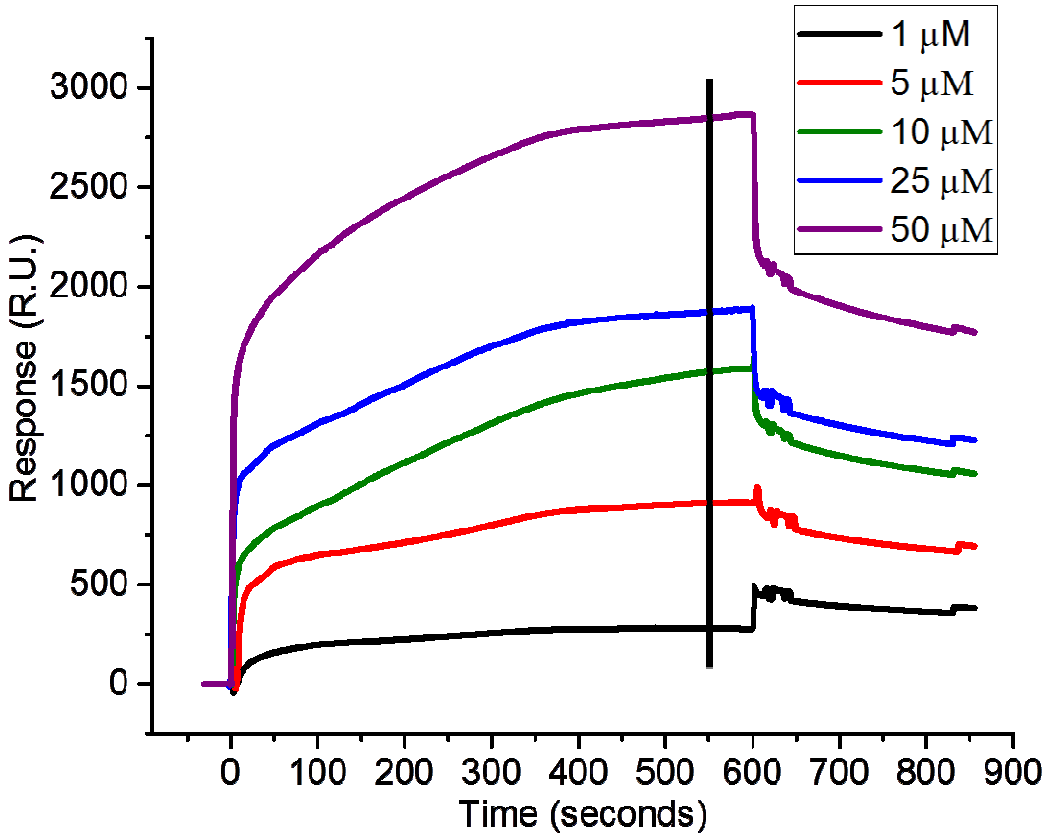

S. Figure 2. Surface plasmon resonance concentration dependence curves of Sar1 interaction with immobilized DOPC liposomes. The graph shows the concentration dependence of Sar1 binding to immobilized DOPC liposomes. The experiment was repeated three times, using a different preparation of Sar1 to generate the global fit shown in Fig. 3b. Some Sar1 desorption can be observed after washing with buffer at t = 600 s.

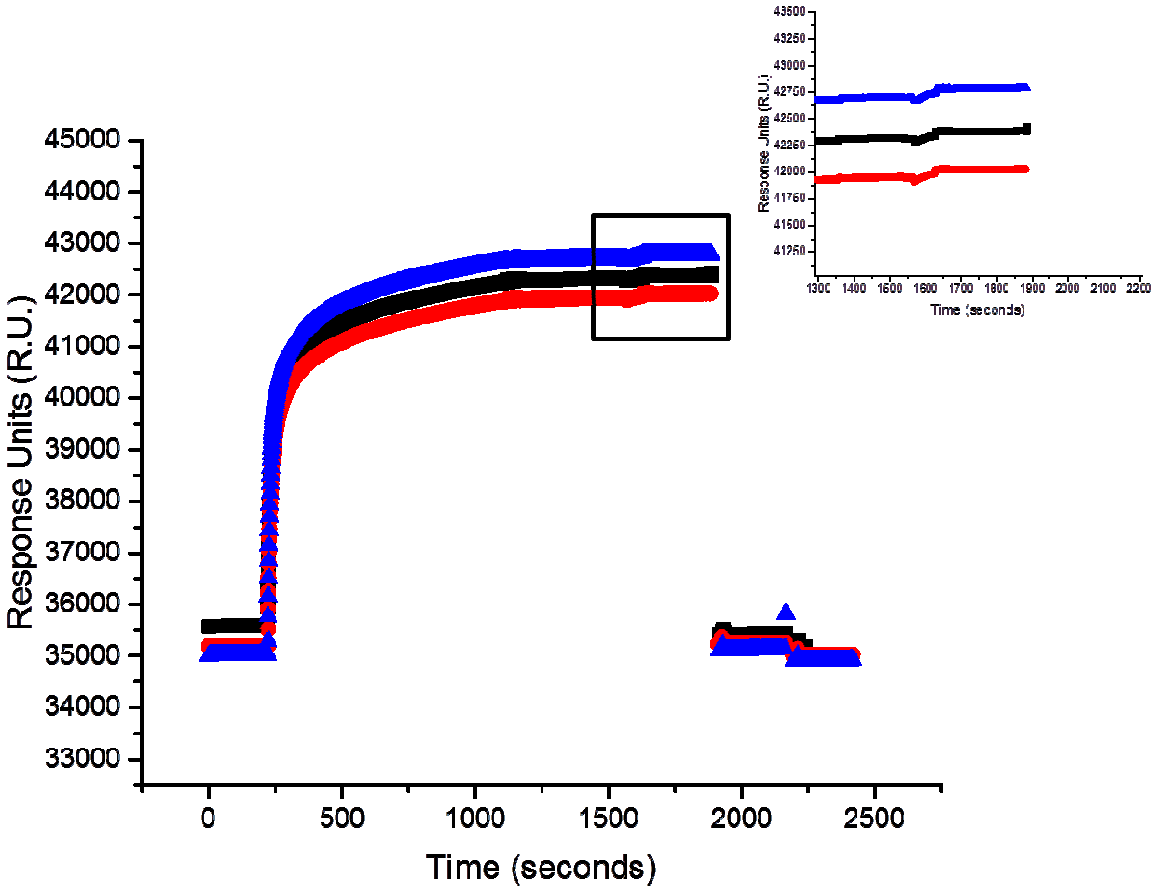

S. Figure 3. BSA injection onto L1 sensor chips covered to saturation with immobilized DOPC liposomes. The injection of DOPC liposomes shows immobilization of BSA at 78 R.U. ± 11, indicating saturation of coverage on the L1 chip is sufficient for monitoring Sar1 binding. The chip was able to be regenerated and reused for each experiment.

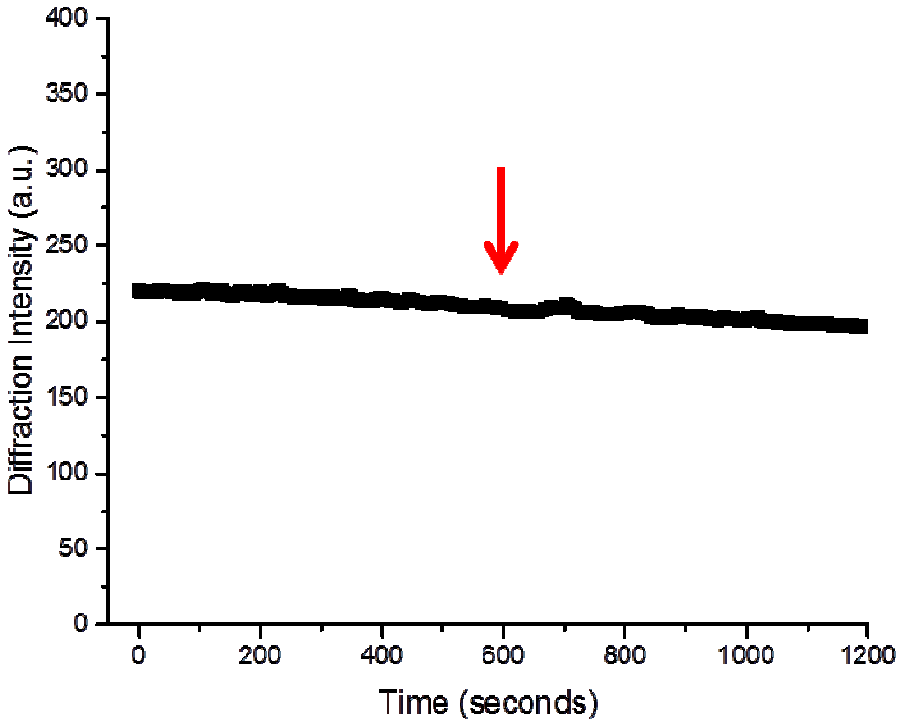

S. Figure 4. Adding LSB to the lipid multilayer gratings with no Sar1 present does not change the diffraction intensity. (a) Graph showing that the diffraction intensity is not affected when SPR running buffer, lacking Sar1, is added to the fluid surrounding the lipid multilayer grating. This demonstrates that Sar1 is responsible for any increase in lipid multilayer diffraction intensity. Some drift in the signal by 25 a.u. can be noted over the time of the experiment.

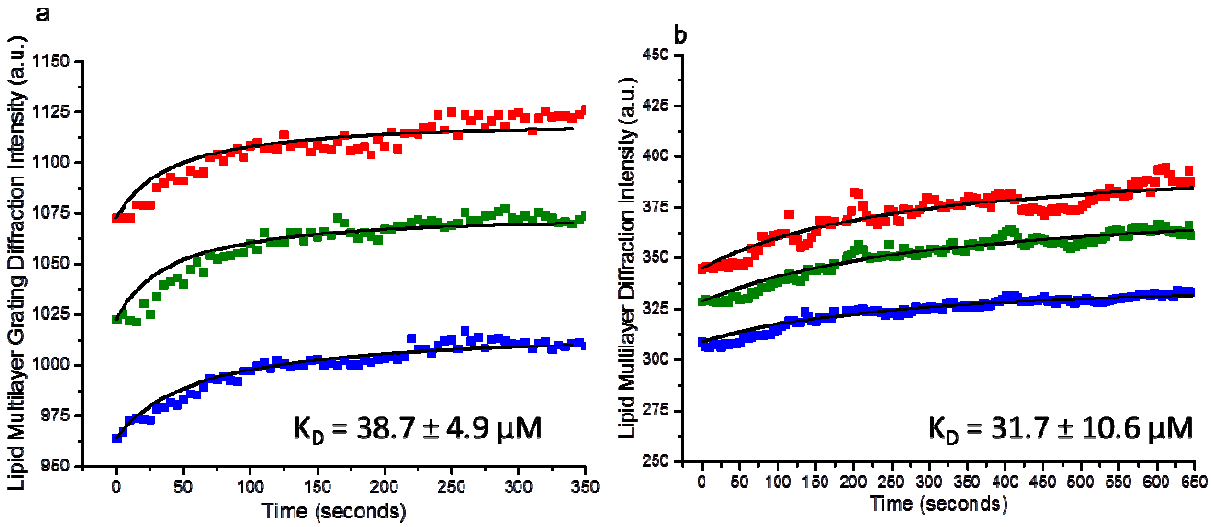

S.Figure 5. **A comparison between Sar1 activity using lipid multilayer gratings of different compositons.** (a) Modeled fits to lipid multilayer grating composed of DOPC:DOPS:cholesterol binding to 10 µM Sar1. The signal increases to saturation after about 350 seconds, then begins the familiar decreasing. 0-350 seconds was modeled and Sar1 affinity was measured to be K_D = 38.7 ± 4.9 µM. (b) Similar to (a), but this time affinity measurements were calculated using purely DOPC gratings. Notably, the kinetics are diminished, reaching saturation after twice the amount of incubation time, however, the affinity was measured to be similar, K_D = 31.7 ± 10.6 µM.

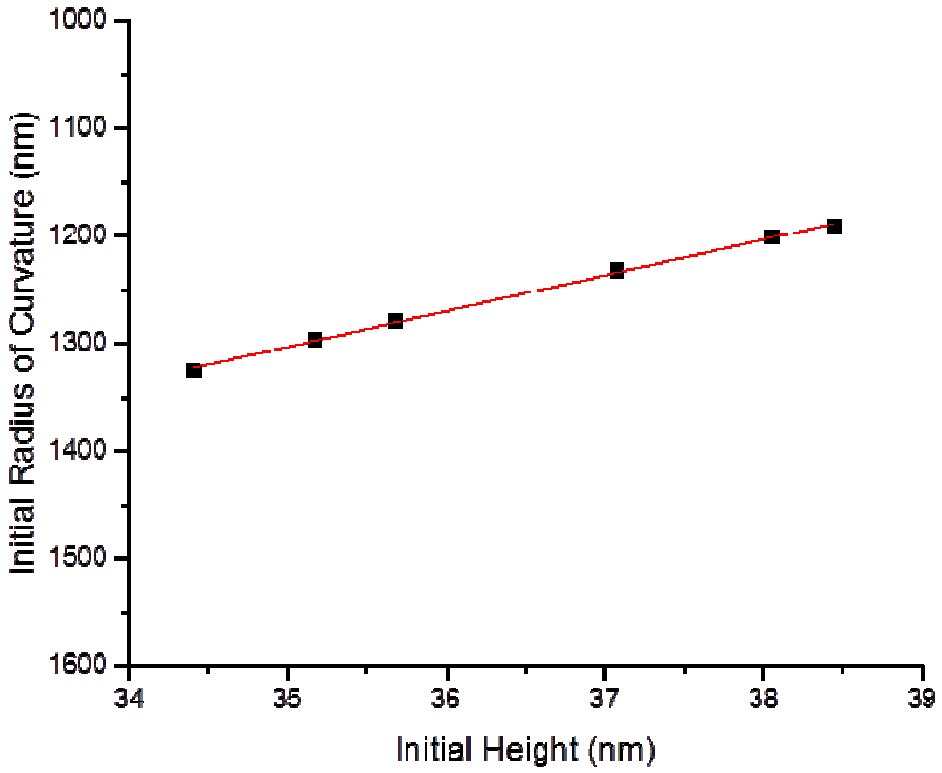

S. Figure 6. Initial curvature of the lipid multilayer gratings. Referring to Fig. 3**,** using the cross-section of the lipid multilayer geometry, the radius of curvature of the lipid grating lines on the surface is related to the width and height of the lipid gratings by the following equation,

$$R_c = \frac{(h^2 + w^2)}{2 * h} \quad \text{(S1)}$$

where h is the height of the lipid grating lines from the surface and w is the width of the line.